

Synthesis and Spectroscopic Characterization of μ_4 -S-Containing Double- and Triple-Butterfly Iron Carbonyl Complexes. Crystal Structures of $[(\mu\text{-EtTe})\text{Fe}_2(\text{CO})_6]_2(\mu_4\text{-S})$, $(\mu\text{-PhS})[\mu\text{-Cp}(\text{CO})_2\text{FeSC}=\text{S}][\text{Fe}_2(\text{CO})_6]_2(\mu_4\text{-S})$, and $(\mu\text{-}p\text{-MeC}_6\text{H}_4\text{S})[\mu\text{-Cp}(\text{CO})_2\text{FeS}][\text{Fe}_2(\text{CO})_6]_3(\mu_4\text{-S})_2$

Li-Cheng Song,^{*,†} Qing-Mei Hu,^{†,‡} Bao-Wei Sun,[†] Ming-Yi Tang,[†] Jing Yang,[†] and Yu-Juan Hua[†]

Department of Chemistry, State Key Laboratory of Elemento-Organic Chemistry, Nankai University, Tianjin 300071, China, and State Key Laboratory of Structural Chemistry, Fuzhou, 350002, China

Received December 5, 2001

We first investigated the nucleophilic reactivities of the complex anions $[(\mu\text{-RTe})(\mu\text{-CO})\text{Fe}_2(\text{CO})_6]^-$ (**1**), $\{(\mu\text{-RS})(\mu\text{-S}=\text{CS})[\text{Fe}_2(\text{CO})_6]_2(\mu_4\text{-S})\}^-$ (**3**), and $\{(\mu\text{-RS})(\mu\text{-S})[\text{Fe}_2(\text{CO})_6]_3(\mu_4\text{-S})_2\}^-$ (**5**) toward the electrophiles SCl_2 and $\text{Cp}(\text{CO})_2\text{FeI}$, respectively. Interestingly, while anions **1** undergo a new type of double nucleophilic substitution reaction with SCl_2 to give the series of one- μ_4 -S-containing double-butterfly iron carbonyl complexes $[(\mu\text{-RTe})\text{Fe}_2(\text{CO})_6]_2(\mu_4\text{-S})$ (**2a**, $\text{R} = \text{Et}$; **2b**, $\text{R} = \text{Ph}$; **2c**, $\text{R} = p\text{-MeC}_6\text{H}_4$; **2d**, $\text{R} = o\text{-MeC}_6\text{H}_4$; **2e**, $\text{R} = \alpha\text{-C}_{10}\text{H}_7$), the single nucleophilic substitution reactions of anions **3** and **5** with $\text{Cp}(\text{CO})_2\text{FeI}$ afford the one- μ_4 -S-containing double-butterfly iron carbonyl complexes $(\mu\text{-RS})[\mu\text{-Cp}(\text{CO})_2\text{FeSC}=\text{S}][\text{Fe}_2(\text{CO})_6]_2(\mu_4\text{-S})$ (**4a**, $\text{R} = \text{Me}$; **4b**, $\text{R} = \text{Et}$; **4c**, $\text{R} = \text{Ph}$; **4d**, $\text{R} = p\text{-MeC}_6\text{H}_4$) and the two- μ_4 -S-containing triple-butterfly iron carbonyl complexes $(\mu\text{-RS})[\mu\text{-Cp}(\text{CO})_2\text{FeS}][\text{Fe}_2(\text{CO})_6]_3(\mu_4\text{-S})_2$ (**6a**, $\text{R} = \text{Me}$; **6b**, $\text{R} = \text{Ph}$; **6c**, $\text{R} = p\text{-MeC}_6\text{H}_4$), respectively. All the new complexes **2a–e**, **4a–d**, and **6a–c** have been characterized by elemental analysis and IR and ^1H NMR spectroscopy, **2a–e** have been characterized as well by ^{125}Te NMR spectroscopy, and **2a**, **4c**, and **6c** have been characterized by crystal X-ray diffraction techniques.

Introduction

In 1967, Dahl and co-workers prepared the first μ_4 -S-containing double-butterfly iron carbonyl complex $[(\mu\text{-MeS})\text{Fe}_2(\text{CO})_6]_2(\mu_4\text{-S})$ in $\sim 1\%$ yield.¹ Later on, Carleton² and Glidewell³ also prepared this μ_4 -S-containing compound by other methods, but the yield is still very low (13% and $\sim 1\%$, respectively). In 1990 de Beer and co-workers⁴ prepared another μ_4 -S-containing double-butterfly iron carbonyl complex, $[(\mu\text{-}t\text{-BuS})\text{Fe}_2(\text{CO})_6]_2(\mu_4\text{-S})$, in 5% yield; however, to our knowledge, no other μ_4 -S-containing butterfly iron carbonyl complexes had been known before 1988, when we reported a general and convenient procedure for the synthesis of such double-butterfly complexes with the general formula $[(\mu\text{-RS})\text{Fe}_2(\text{CO})_6]_2(\mu_4\text{-S})$ ($\text{R} = \text{Me}, \text{Et}, \text{PhCH}_2, p\text{-MeC}_6\text{H}_4, \text{PhC}\equiv\text{C}$) in high yield (61–91%).⁵ In view of the novelty and diversity of structures and reactivities of μ_4 -S-containing iron carbonyl complexes, we have been

interested in studying both μ_4 -S-forming reactions and the reactions with μ_4 -S-containing reactive intermediates, which has so far led us to obtain a great variety of double-, triple-, and even multiple-butterfly iron carbonyl complexes.^{6–10} This article will describe a new type of μ_4 -S-forming reaction to give the series of double-butterfly complexes $[(\mu\text{-RTe})\text{Fe}_2(\text{CO})_6]_2(\mu_4\text{-S})$, and the nucleophilic reactions of the μ_4 -S-containing anionic intermediates $\{(\mu\text{-RS})(\mu\text{-S}=\text{CS})[\text{Fe}_2(\text{CO})_6]_2(\mu_4\text{-S})\}^-$ and $\{(\mu\text{-RS})(\mu\text{-S})[\text{Fe}_2(\text{CO})_6]_3(\mu_4\text{-S})_2\}^-$ to afford the double- and triple-butterfly complexes $(\mu\text{-RS})[\mu\text{-Cp}(\text{CO})_2\text{FeSC}=\text{S}][\text{Fe}_2(\text{CO})_6]_2(\mu_4\text{-S})$ and $(\mu\text{-RS})[\mu\text{-Cp}(\text{CO})_2\text{FeS}][\text{Fe}_2(\text{CO})_6]_3(\mu_4\text{-S})_2$. In addition, structural characterizations of these new μ_4 -S-containing complexes, particularly by X-ray diffraction techniques, are also described.

Results and Discussion

Syntheses via Reactions of the Anions $[(\mu\text{-RTe})(\mu\text{-CO})\text{Fe}_2(\text{CO})_6]^-$ (**1**) and Characterization of $[(\mu\text{-$

* To whom correspondence should be addressed. Fax: +86-22-23504853. E-mail: lcsong@public.tpt.tj.cn.

[†] Nankai University.

[‡] State Key Laboratory of Structural Chemistry.

(1) Coleman, J. M.; Wojcicki, A.; Pollick, P. J.; Dahl, L. F. *Inorg. Chem.* **1967**, *6*, 1236.

(2) Carleton, S. C.; Kennedy, F. G.; Knox, S. A. R. *J. Chem. Soc., Dalton Trans.* **1981**, 2230.

(3) Glidewell, C.; Hyde, A. R. *Inorg. Chim. Acta* **1984**, *87*, L15.

(4) de Beer, J. A.; Haines, R. J. *J. Organomet. Chem.* **1970**, *24*, 757.

(5) Song, L.-C.; Kadiata, M.; Wang, J.-T.; Wang, R.-J.; Wang, H.-G. *J. Organomet. Chem.* **1988**, *340*, 239.

(6) Song, L.-C.; Yan, C.-G.; Hu, Q.-M.; Wang, R.-J.; Mak, T. C. W.; Huang, X.-Y. *Organometallics* **1996**, *15*, 1535.

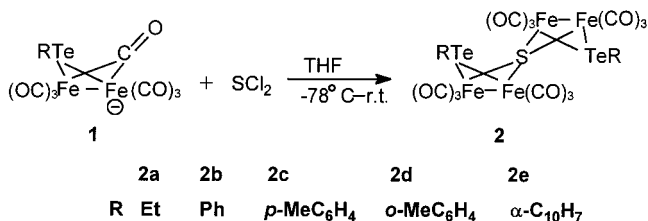
(7) Song, L.-C.; Qin, X.-D.; Hu, Q.-M.; Huang, X.-Y. *Organometallics* **1998**, *17*, 5437.

(8) Song, L.-C.; Lu, G.-L.; Hu, Q.-M.; Fan, H.-T.; Chen, Y.; Sun, J. *Organometallics* **1999**, *18*, 3258.

(9) Song, L.-C.; Hu, Q.-M.; Fan, H.-T.; Sun, B.-W.; Tang, M.-Y.; Chen, Y.; Sun, Y.; Sun, C.-X.; Wu, Q.-J. *Organometallics* **2000**, *19*, 3909.

(10) Song, L.-C.; Lu, G.-L.; Hu, Q.-M.; Yang, J.; Sun, J. *J. Organomet. Chem.* **2001**, *623*, 56.

Scheme 1



RTeFe₂(CO)₆]₂(μ₄-S) (2a–e). Crystal Structure of 2a (R = Et). We found that the [MgBr]⁺ salts of anions **1**, formed from an insertion reaction of elemental Te with Grignard reagents RMgBr followed by reaction of the intermediates RTeMgBr with Fe₃(CO)₁₂,¹¹ could react with an excess amount of SCl₂ from –78 °C to room temperature in THF, through a type of μ₄-S-forming reaction to give the series of μ₄-S-containing double-butterfly iron carbonyl complexes **2a–e** (Scheme 1).

It is worth pointing out that both the μ₄-S-forming reaction of **1** with SCl₂ and the μ₄-S-containing double-butterfly Fe₄Te₂(μ₄-S) products **2a–e** are new, although the μ₄-S-containing analogues with a double-butterfly core Fe₄S₂(μ₄-S)^{1–5} and Fe₄Se₂(μ₄-S)⁶ and the corresponding μ₄-S-forming reactions^{1–6} were previously reported. Complexes **2a–e** have been characterized by combustion analysis and IR, ¹H NMR, and ¹²⁵Te NMR spectroscopy, as well as by X-ray diffraction techniques. ¹²⁵Te NMR spectroscopy has been developed as an important tool for characterizing Te-containing organometallic compounds.^{12–14} We found that the ¹²⁵Te NMR spectra of **2a–e** each displayed a singlet in the region 168.5–309.5 ppm for their two bridged identical Te atoms. The ¹²⁵Te NMR resonance signal of **2a** (168.5 ppm) appeared at much higher field than those of **2b–e** (242.3–309.5 ppm), which is obviously due to the fact that the Et group in **2a** is an electron-donating group, whereas the aromatic R groups in **2b–e** are electron-withdrawing.

It is noteworthy that the reaction of the [MgBr]⁺ salts of anions **1** with SCl₂ also afforded the corresponding single-butterfly complexes (μ-RTe)₂Fe₂(CO)₆. This is not surprising, since reactions involving anions of type **1** were previously reported to produce the same type of complexes (μ-RTe)₂Fe₂(CO)₆, possibly generated through decomposition of anions **1** followed by dimerization of the intermediate fragment (μ-RTe)Fe(CO)₃.¹⁵ The known complexes (μ-RTe)₂Fe₂(CO)₆ (R = Et,¹¹ Ph,^{15,16} *p*-MeC₆H₄,¹⁵ *o*-MeC₆H₄¹⁵) were identified by comparison of their IR and ¹H NMR spectra with those of authentic samples, whereas the new complex (R = α-C₁₀H₇) was characterized by C/H analysis and IR and ¹H NMR spectroscopy.

The mechanism for the μ₄-S-forming reaction to produce the double-butterfly complexes **2a–e** can be

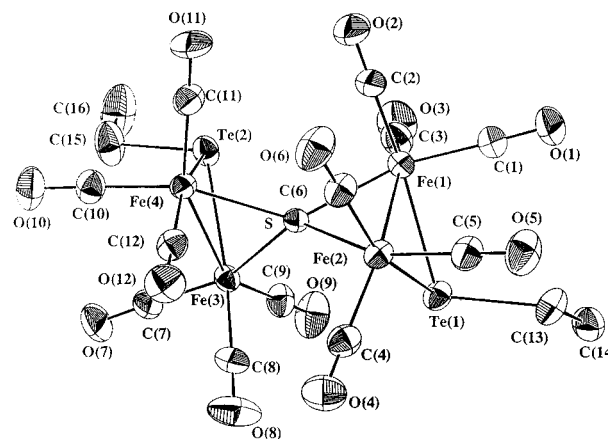


Figure 1. ORTEP drawing of **2a** with atom-labeling scheme.

Scheme 2

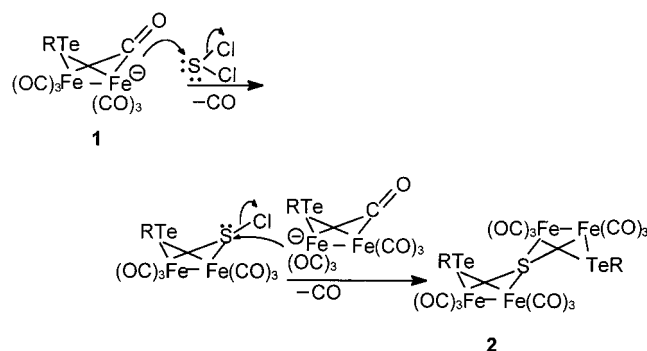


Table 1. Selected Bond Lengths (Å) and Angles (deg) for **2a**

Te(1)–Fe(2)	2.546(2)	Te(1)–Fe(1)	2.563(1)
Te(2)–Fe(4)	2.533(2)	Te(2)–Fe(3)	2.555(1)
Fe(4)–S	2.241(2)	Fe(1)–S	2.248(2)
Fe(2)–S	2.240(2)	Fe(1)–Fe(2)	2.572(2)
Fe(3)–S	2.243(2)	Fe(3)–Fe(4)	2.577(2)
Fe(4)–S–Fe(3)	70.17(6)	Fe(3)–S–Fe(1)	129.15(8)
Fe(4)–S–Fe(2)	129.32(8)	Fe(1)–S–Fe(2)	69.93(6)
Fe(1)–Te(1)–Fe(2)	60.45(4)	Fe(3)–Te(2)–Fe(4)	60.86(4)
S–Fe(1)–Te(1)	78.82(6)	S–Fe(1)–Fe(2)	54.88(5)
S–Fe(3)–Te(2)	78.98(5)	S–Fe(3)–Fe(4)	54.87(5)
Te(2)–Fe(3)–Fe(4)	59.14(4)	Te(1)–Fe(1)–Fe(2)	59.45(4)

proposed on the basis of similarity with the reactions of anions **1** with other electrophiles¹¹ (Scheme 2). Apparently, this mechanism involves a double nucleophilic attack of the negatively charged Fe atom in **1** at the S atom in SCl₂ to eliminate two Cl[–] anions and a double coordination of the lone electron pairs on the S atom to the neighboring Fe atoms with concomitant loss of two μ-CO ligands.

To unequivocally confirm the double-butterfly structures of the products obtained from the above new type of reaction, a single-crystal X-ray diffraction analysis for [(μ-EtTe)Fe₂(CO)₆]₂(μ₄-S) (**2a**) was performed. While Figure 1 shows its structure, Table 1 lists the selected bond lengths and angles. The X-ray diffraction study revealed that **2a** consists of the two butterfly cores Fe(1)Fe(2)Te(1)S and Fe(3)Fe(4)Te(2)S joined to a spiro type of S atom, the dihedral angle between Fe(1)–Fe(2)–S and Fe(3)–Fe(4)–S is 96.6°, each Fe atom

(11) Song, L.-C.; Lu, G.-L.; Hu, Q.-M.; Qin, X.-D.; Sun, C.-X.; Yang, J.; Sun, J. *J. Organomet. Chem.* **1998**, 571, 55.

(12) Bogan, L. E.; Clark, G. R.; Rauchfuss, T. B. *Inorg. Chem.* **1986**, 25, 4050.

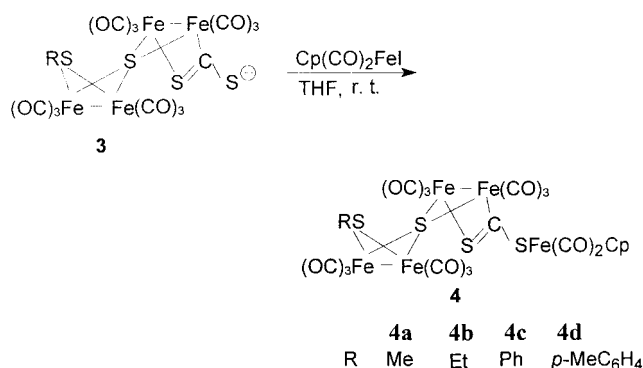
(13) Bochman, R. E.; Whitmire, K. H. *Organometallics* **1993**, 12, 1988.

(14) Song, L.-C.; Shi, Y.-C.; Zhu, W.-F.; Hu, Q.-M.; Huang, X.-Y.; Du, F.; Mao, X.-A. *Organometallics* **2000**, 19, 156.

(15) Song, L.-C.; Yan, C.-G.; Hu, Q.-M.; Huang, X.-Y. *Organometallics* **1997**, 16, 3769.

(16) Schermer, E. D.; Baddley, W. H. *J. Organomet. Chem.* **1971**, 30, 67.

Scheme 3



carries three terminal carbonyls, and both Te atoms are attached to Et groups by an equatorial type of bond.¹⁷ Thus, this structure is completely similar to those of its analogues $[(\mu\text{-MeS})\text{Fe}_2(\text{CO})_6]_2(\mu_4\text{-S})^1$ and $[(\mu\text{-EtS})\text{Fe}_2(\text{CO})_6]_2(\mu_4\text{-S})^5$. The similarity can be also seen from the comparable parameters between **2a** and its two above-mentioned analogues. For instance, in **2a** the bond lengths Fe(1)–Fe(2) and Fe(3)–Fe(4) are 2.572(2) and 2.577(2) Å, whereas in $[(\mu\text{-EtS})\text{Fe}_2(\text{CO})_6]_2(\mu_4\text{-S})$ the corresponding bond lengths are 2.542(2) and 2.538(2) Å. In addition, in **2a** the bond angles Fe(1)–S–Fe(2) and Fe(3)–S–Fe(4) are 69.93(6) and 70.17(6)°, whereas in the latter the corresponding angles are 69.04(7) and 68.69(7)°. The minor differences in parameters between **2a** and $[(\mu\text{-EtS})\text{Fe}_2(\text{CO})_6]_2(\mu_4\text{-S})$ are apparently due to replacement of the two wing-tip S atoms in the butterfly core of $[(\mu\text{-EtS})\text{Fe}_2(\text{CO})_6]_2(\mu_4\text{-S})$ by two Te atoms.

Syntheses via Reactions of the Anions $\{(\mu\text{-RS})(\mu\text{-S=CS})[\text{Fe}_2(\text{CO})_6]_2(\mu_4\text{-S})\}^-$ (3**) and Characterization of $(\mu\text{-RS})[\mu\text{-Cp}(\text{CO})_2\text{FeSC=S}][\text{Fe}_2(\text{CO})_6]_2(\mu_4\text{-S})$ (**4a–d**). Crystal Structure of **4c** (R = Ph).** Interestingly, we have further found that the novel $\mu_4\text{-S}$ -containing anionic intermediates **3**, which were prepared as their $[\text{MgX}]^+$ (X = Br, I) salts from a sequential reaction of $\mu\text{-S}_2\text{Fe}_2(\text{CO})_6$ with the Grignard reagents RMgX , $\text{Fe}_3(\text{CO})_{12}$, and CS_2 ,⁹ could undergo nucleophilic substitution reactions with $\text{Cp}(\text{CO})_2\text{FeI}$ in THF at room temperature, affording the S-functionalized double-butterfly iron carbonyl complexes **4a–d**, as shown in Scheme 3.

Complexes **4a–d** were characterized by elemental analysis, spectroscopy, and X-ray crystal diffraction analysis. For example, the IR spectra of **4a–d** showed one absorption band in the region 1020–999 cm^{-1} for the coordinated C=S double bond,¹⁸ whereas the ^1H NMR spectra of **4a–d** exhibited a singlet in the range 5.03–5.38 ppm for their Cp groups. To unambiguously confirm the double-butterfly structures of the products generated from anions **3**, a single-crystal X-ray diffraction analysis for $(\mu\text{-PhS})[\mu\text{-Cp}(\text{CO})_2\text{FeSC=S}][\text{Fe}_2(\text{CO})_6]_2(\mu_4\text{-S})$ (**4c**) was undertaken. The molecular structure of **4c** is shown in Figure 2, whereas its selected bond lengths and angles are given in Table 2. The X-ray diffraction study showed that **4c** consists of the two butterfly subcluster cores Fe(1)Fe(2)S(1)S(2) and Fe(3)Fe(4)S(1)C(15)S(3) joined to a spiro type of S(1)

atom. The dihedral angle between Fe(1)–Fe(2)–S(1) and Fe(3)–Fe(4)–S(1) is 97.1°, while the S(2) atom is bonded to C(16) of the phenyl group by an equatorial type of bond.¹⁷ The S(4) atom is bound to C(15) as well as Fe(5) of the $\text{Cp}(\text{CO})_2\text{Fe}$ group; in addition, all 12 carbonyls attached to the Fe(1)–Fe(5) atoms are terminal. The geometric parameters of **4c** are similar to those of its analogue $(\mu\text{-MeS})(\mu\text{-MeSC=S})[\text{Fe}_2(\text{CO})_6]_2(\mu_4\text{-S})$.⁹ For example, in **4c** the bond lengths Fe(1)–Fe(2) and Fe(3)–Fe(4) are 2.5356(6) and 2.6234(5) Å, whereas in $(\mu\text{-MeS})(\mu\text{-MeSC=S})[\text{Fe}_2(\text{CO})_6]_2(\mu_4\text{-S})$ the corresponding lengths are 2.5376(8) and 2.6496(7) Å. In addition, in **4c** the coordinated thiocarbonyl C(15)=S(3) is 1.671(3) Å, whereas the corresponding thiocarbonyl in $(\mu\text{-MeS})(\mu\text{-MeSC=S})[\text{Fe}_2(\text{CO})_6]_2(\mu_4\text{-S})$ is 1.672(4) Å. Apparently, the coordinated thiocarbonyls in **4c** and $(\mu\text{-MeS})(\mu\text{-MeSC=S})[\text{Fe}_2(\text{CO})_6]_2(\mu_4\text{-S})$ are just slightly longer than the corresponding thiocarbonyl in $(\mu\text{-PhCH}_2\text{SC=S})\text{Fe}_2(\text{CO})_6$ (1.63(1) Å)¹⁹ but are much longer than the uncoordinated C=S double bond in free CS_2 (1.554 Å).²⁰

Syntheses via Reactions of Anions $\{(\mu\text{-RS})(\mu\text{-S})[\text{Fe}_2(\text{CO})_6]_3(\mu_4\text{-S})_2\}^-$ (5**) and Characterization of $(\mu\text{-RS})[\mu\text{-Cp}(\text{CO})_2\text{FeS}][\text{Fe}_2(\text{CO})_6]_3(\mu_4\text{-S})_2$ (**6a–c**). Crystal Structure of **6c** (R = *p*-MeC₆H₄).** More interestingly, we have found that the $[\text{MgX}]^+$ (X = Br, I) salts of the novel two- $\mu_4\text{-S}$ -containing triple-butterfly anions **5**, prepared from the sequential reaction of $\mu\text{-S}_2\text{-Fe}_2(\text{CO})_6$ with the Grignard reagents RMgX , $\text{Fe}_3(\text{CO})_{12}$ and $\mu\text{-S}_2\text{Fe}_2(\text{CO})_6$,⁹ could also undergo nucleophilic substitution reactions with the electrophile $\text{Cp}(\text{CO})_2\text{FeI}$ in THF at room temperature to give the triple-butterfly iron carbonyl complexes **6a–c**, as shown in Scheme 4.

Products **6a–c** were characterized by elemental analysis, spectroscopy, and X-ray crystal diffraction analysis. For example, the IR spectra of **6a–c** displayed three absorption bands in the range 2086–1988 cm^{-1} for their terminal carbonyls, whereas the ^1H NMR spectra of **6a–c** exhibited a singlet at ca. 5.47 ppm for their Cp groups. In principle, the R and $\text{Cp}(\text{CO})_2\text{Fe}$ groups in **6a–c** should be attached to the bridged S atoms by an equatorial type of bond, to avoid the sterically strong repulsions between these groups and the structural moieties axially bonded to their neighboring bridged S atoms.^{6,7} Fortunately, this has been confirmed by crystal X-ray diffraction analysis of **6c**. The molecular structure of **6c** is shown in Figure 3, whereas its selected bond lengths and angles are given in Table 3.

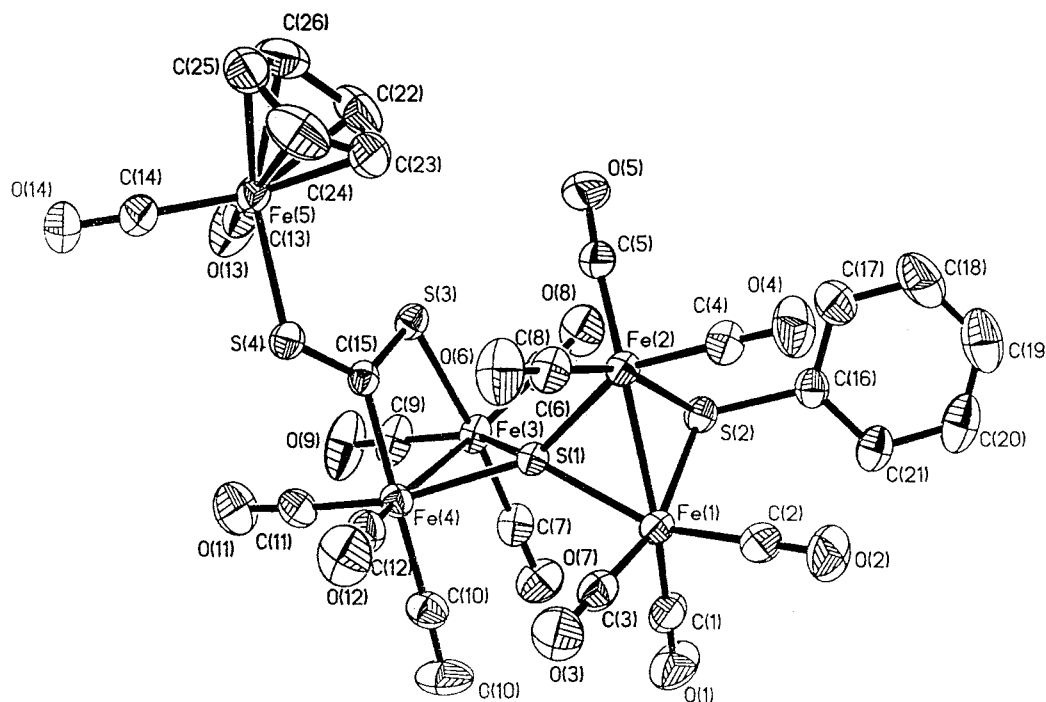
As shown in Figure 3, **6c** contains the three butterfly cores Fe(2)Fe(3)S(1)S(2), Fe(4)Fe(5)S(2)S(3), and Fe(6)Fe(7)S(3)S(4) joined together by two $\mu_4\text{-S}$ atoms of S(2) and S(3). In addition, except for Fe(1) with two terminal carbonyls, each of the Fe atoms from Fe(2) to Fe(7) is linked to three terminal carbonyls, and the $\text{Cp}(\text{CO})_2\text{Fe}$ and *p*-MeC₆H₄ groups are bonded to the bridged S atoms of S(1) and S(4) by an equatorial type of bond, respectively. It is worthy of note that in the three butterfly cores the geometric parameters of the middle core are slightly different from those of the two side cores. For example, the bond length of Fe(2)–Fe(3) (2.5059(11) Å) or Fe(6)–Fe(7) (2.5094(11) Å) is shorter

(17) Shaver, A.; Fitzpatrick, P. J.; Steliou, K.; Butler, I. S. *J. Am. Chem. Soc.* **1979**, *101*, 1313.

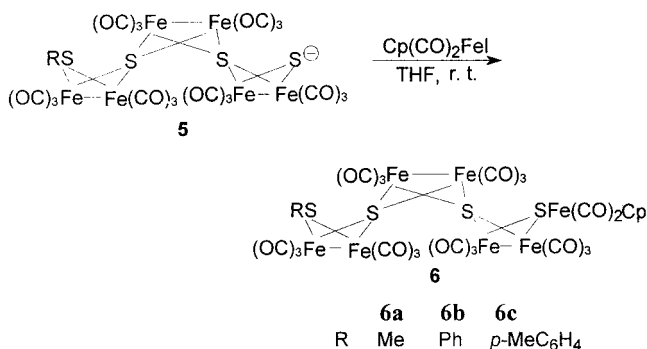
(18) Patin, H.; Mignani, G.; Mahé, C.; Le Marouille, J.-Y.; Southern, T. G.; Benoit, A.; Grandjean, D. *J. Organomet. Chem.* **1980**, *197*, 315.

(19) Song, L.-C.; Yan, C.-G.; Hu, Q.-M.; Wang, R.-J.; Mak, T. C. W. *Organometallics* **1995**, *14*, 5513.

(20) Butler, I. S.; Fenster, A. E. *J. Organomet. Chem.* **1974**, *66*, 161.

**Figure 2.** ORTEP drawing of **4c** with atom-labeling scheme.**Table 2.** Selected Bond Lengths (Å) and Angles (deg) for **4c**

Fe(1)–S(1)	2.2532(7)	Fe(1)–S(2)	2.2748(8)
Fe(1)–Fe(2)	2.5356(6)	Fe(2)–S(1)	2.2480(7)
Fe(2)–S(2)	2.2784(8)	Fe(3)–S(1)	2.2366(7)
Fe(3)–S(3)	2.3119(8)	Fe(3)–Fe(4)	2.6234(5)
Fe(5)–S(4)	2.2631(8)	S(1)–Fe(4)	2.2411(7)
C(15)–S(3)	1.671(3)	C(15)–S(4)	1.683(3)
S(1)–Fe(1)–S(2)	76.57(3)	Fe(3)–S(1)–Fe(4)	71.73(2)
Fe(3)–S(1)–Fe(2)	126.97(3)	Fe(4)–S(1)–Fe(2)	137.08(3)
Fe(3)–S(1)–Fe(1)	133.41(3)	S(1)–Fe(2)–Fe(1)	55.81(2)
S(1)–Fe(1)–Fe(2)	55.62(2)	S(2)–Fe(2)–Fe(1)	56.09(2)
S(2)–Fe(1)–Fe(2)	56.23(2)	S(1)–Fe(2)–S(2)	76.60(3)
Fe(1)–S(2)–Fe(2)	67.68(2)	Fe(4)–S(1)–Fe(1)	130.85(3)
S(3)–Fe(3)–Fe(4)	75.67(2)	S(1)–Fe(4)–Fe(3)	54.056(19)

Scheme 4

than that of Fe(4)–Fe(5) (2.5684(11) Å), and the dihedral angle between Fe(2)–Fe(3)–S(1) and Fe(2)–Fe(3)–(2) (85.02°) or Fe(6)–Fe(7)–S(3) and Fe(6)–Fe(7)–S(4) (84.00°) is larger than that between Fe(4)–Fe(5)–S(2) and Fe(4)–Fe(5)–S(3) (73.53°). In fact, the basic geometric parameters of **6c** are comparable with those of the butterfly Fe/S cluster complexes, such as $[(\mu\text{-PhS})\text{Fe}_2(\text{CO})_6(\mu\text{-S})]_2^{21}$ and $(\mu\text{-PhCH}_2\text{S})_2[\text{Fe}_2(\text{CO})_6]_3^{22}$ ($\mu_4\text{-S}$).⁹

Experimental Section

General Comments. All reactions were carried out under an atmosphere of prepurified nitrogen using standard Schlenk and vacuum-line techniques. Tetrahydrofuran (THF) was distilled from Na/benzophenone ketyl under nitrogen. $\text{Fe}_3(\text{CO})_{12}$,²² $\mu\text{-S}_2\text{Fe}_2(\text{CO})_6$,²³ the Grignard reagents RMgX ,²⁴ SCl_2 ,²⁵ and $\text{Cp}(\text{CO})_2\text{FeI}$ ²⁶ were prepared according to literature procedures, whereas the others used in this paper were of commercial origin and used without further purification. Preparative TLC was carried out on glass plates (26 × 20 × 0.25 cm) coated with silica gel H (10–40 μm). IR spectra were recorded on a Nicolet 170SX FT-IR or Bruker Vector 22 infrared spectrophotometer. ¹H NMR spectra were recorded on a Bruker AC-P 200 NMR spectrometer. ¹²⁵Te NMR spectra were recorded on a Varian Unity-Plus 400 NMR spectrometer with Ph_2Te_2 as external standard, and the chemical shifts are referenced to Me_2Te (δ 0). C/H analyses were performed on a Yanaco CHN Corder MT-3 analyzer or a Elementar Vario EL analyzer. Melting points were determined on a Yanaco MP-500 apparatus and were uncorrected.

Standard in Situ Preparation of $[\text{MgBr}]^+$ Salts of the Anions $[(\mu\text{-RTe})(\mu\text{-CO})\text{Fe}_2(\text{CO})_6]^-$ (1**).** A 100 mL two-necked flask equipped with a stir bar, a serum cap, and a reflux condenser topped with a nitrogen inlet tube was charged with 0.511 g (4.0 mmol) of tellurium powder, 25 mL of THF, and 4.0 mmol of RMgBr (R = Et, Ph, *p*-MeC₆H₄, *o*-MeC₆H₄, $\alpha\text{-C}_{10}\text{H}_7$) in Et₂O. The mixture was refluxed for 2 h to give a slight gray solution of RTeMgBr . When the solution was cooled to room temperature, 2.0 g (3.96 mmol) of $\text{Fe}_3(\text{CO})_{12}$ was added and the reaction mixture was stirred for ca. 0.5 h to produce a brown-red solution containing the salt of **1**[MgBr] (R = Et,

(21) Seyferth, D.; Kiwan, A. M.; Sinn, E. *J. Organomet. Chem.* **1985**, *281*, 111.

(22) King, R. B. *Organometallic Syntheses; Transition-Metal Compounds*, Academic Press: New York, 1965; Vol. 1, p 95.

(23) Seyferth, D.; Henderson, R. S.; Song, L.-C. *Organometallics* **1982**, *1*, 125.

(24) Gilman, H.; Zoellner, E. A.; Dickey, J. B. *J. Am. Chem. Soc.* **1929**, *51*, 1576.

(25) Brauer, G. *Handbook of Preparative Inorganic Chemistry*, 2nd ed.; Academic Press: New York, 1963; Vol. 1, p 371.

(26) King, R. B. *Organometallic Syntheses; Transition-Metal Compounds*, Academic Press: New York, 1965; Vol. 1, p 175.

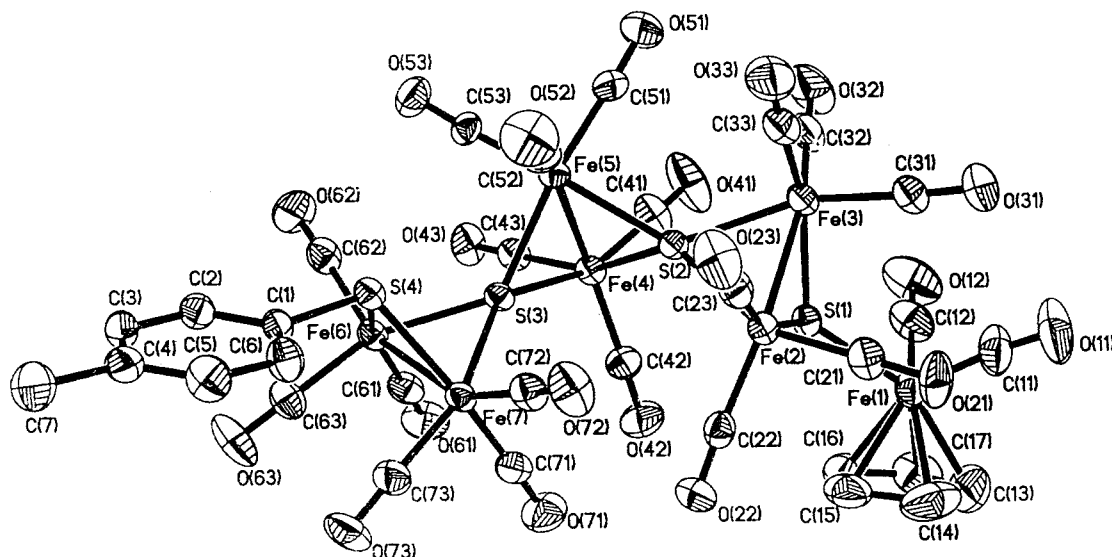


Figure 3. ORTEP drawing of **6c** with atom-labeling scheme.

Table 3. Selected Bond Lengths (Å) and Angles (deg) for **6c**

Fe(1)–S(1)	2.3008(18)	S(1)–Fe(2)	2.2806(16)
Fe(2)–S(2)	2.2827(15)	Fe(2)–Fe(3)	2.5059(11)
Fe(7)–S(3)	2.2632(14)	Fe(7)–S(4)	2.2769(17)
Fe(3)–S(2)	2.2809(15)	Fe(3)–S(1)	2.2887(17)
Fe(4)–S(3)	2.2492(15)	S(2)–Fe(4)	2.2642(15)
Fe(4)–Fe(5)	2.5684(11)	Fe(6)–Fe(7)	2.5094(11)
S(3)–Fe(6)–S(4)	76.55(5)	S(3)–Fe(6)–Fe(7)	56.29(4)
S(4)–Fe(6)–Fe(7)	56.63(4)	S(3)–Fe(7)–S(4)	76.50(5)
S(3)–Fe(7)–Fe(6)	56.44(4)	S(4)–Fe(7)–Fe(6)	56.39(4)
Fe(2)–S(1)–Fe(3)	66.52(5)	Fe(2)–S(1)–Fe(1)	125.02(7)
Fe(3)–S(1)–Fe(1)	131.15(7)	Fe(5)–S(2)–Fe(4)	69.12(5)
Fe(5)–S(2)–Fe(3)	129.27(6)	Fe(4)–S(2)–Fe(3)	129.37(7)

Ph, *p*-MeC₆H₄, *o*-MeC₆H₄, α -C₁₀H₇), which was employed immediately in the preparations of **2a–e**.

Preparation of $[(\mu\text{-EtTe})\text{Fe}_2(\text{CO})_6]_2(\mu_4\text{-S})$ (2a**).** To the above prepared solution of **1**[MgBr] (R = Et), which had been cooled to -78°C by a dry ice/acetone bath, was added 0.10 mL (1.5 mmol) of SCl₂, and this mixture was stirred for 20 min. After the dry ice/acetone bath was removed, the mixture was naturally warmed to room temperature and then continued to be stirred for 4 h. The solvent was removed under reduced pressure. The residue was subjected to TLC separation using CH₂Cl₂/petroleum ether (v/v = 1:20) as eluent. From the first main red band was obtained 0.289 g (24%) of $(\mu\text{-EtTe})_2\text{Fe}_2(\text{CO})_6$.¹¹ The second main brown-red band afforded 0.129 g (10%) of **2a** as a red solid. Mp: 113.5°C dec. Anal. Calcd for C₁₆H₁₀Fe₄O₁₂STe₂: C, 21.24; H, 1.11. Found: C, 20.97; H, 1.00. IR (KBr disk): $\nu_{\text{C=O}}$ 2090 (m), 2046 (s), 2042 (vs), 1981 (vs) cm⁻¹. ¹H NMR (CDCl₃): 1.50–1.64 (m, 6H, 2CH₃), 2.75–2.85 (m, 4H, 2CH₂) ppm. ¹²⁵Te NMR (CDCl₃): 168.5 (s) ppm.

Preparation of $[(\mu\text{-PhTe})\text{Fe}_2(\text{CO})_6]_2(\mu_4\text{-S})$ (2b**).** The same procedure as that for **2a** was followed, but **1**[MgBr] (R = Ph) was used instead of **1**[MgBr] (R = Et). From the first main orange-red band was obtained 0.202 g (15%) of $(\mu\text{-PhTe})_2\text{Fe}_2(\text{CO})_6$.¹⁵ The second main orange-red band afforded 0.304 g (20%) of **2b** as a red solid. Mp: 202°C dec. Anal. Calcd for C₂₄H₁₀Fe₄O₁₂STe₂: C, 28.80; H, 1.01. Found: C, 28.65; H, 1.14. IR (KBr disk): $\nu_{\text{C=O}}$ 2082 (s), 2044 (vs), 2026 (vs), 1985 (vs), 1966 (vs) cm⁻¹. ¹H NMR (acetone-*d*₆): 7.10–7.64 (m, 10H, 2C₆H₅) ppm. ¹²⁵Te NMR (CDCl₃): 309.5 (s) ppm.

Preparation of $[(\mu\text{-}p\text{-MeC}_6\text{H}_4\text{Te})\text{Fe}_2(\text{CO})_6]_2(\mu_4\text{-S})$ (2c**).** The same procedure as that for **2a** was followed, but **1**[MgBr] (R = *p*-MeC₆H₄) was used instead of **1**[MgBr] (R = Et). From the first main red band was obtained 0.521 g (36%) of $(\mu\text{-}p\text{-MeC}_6\text{H}_4\text{Te})_2\text{Fe}_2(\text{CO})_6$.¹⁵ The second main dark red band af-

forded 0.324 g (21%) of **2c** as a dark red solid. Mp: 215°C dec. Anal. Calcd for C₂₆H₁₄Fe₄O₁₂STe₂: C, 30.34; H, 1.37. Found: C, 30.30; H, 1.24. IR (KBr disk): $\nu_{\text{C=O}}$ 2074 (s), 2045 (s), 2034 (vs), 1989 (vs), 1970 (vs) cm⁻¹. ¹H NMR (acetone-*d*₆): 2.30 (s, 6H, 2CH₃), 7.30 (q, AA'BB', *J* = 7.8 Hz, 8H, 2C₆H₄) ppm. ¹²⁵Te NMR (CDCl₃): 306.3 (s) ppm.

Preparation of $[(\mu\text{-}o\text{-MeC}_6\text{H}_4\text{Te})\text{Fe}_2(\text{CO})_6]_2(\mu_4\text{-S})$ (2d**).** The same procedure as that for **2a** was followed, but **1**[MgBr] (R = *o*-MeC₆H₄) was used instead of **1**[MgBr] (R = Et). From the first main orange-red band was obtained 0.240 g (17%) of $(\mu\text{-}o\text{-MeC}_6\text{H}_4\text{Te})_2\text{Fe}_2(\text{CO})_6$.¹⁵ The second main brown-red band afforded 0.318 g (21%) of **2d** as a red solid. Mp: 216°C dec. Anal. Calcd for C₂₆H₁₄Fe₄O₁₂STe₂: C, 30.34; H, 1.37. Found: C, 30.36; H, 1.45. IR (KBr disk): $\nu_{\text{C=O}}$ 2082 (s), 2026 (vs), 2010 (s), 1989 (vs), 1973 (vs), 1958 (vs) cm⁻¹. ¹H NMR (acetone-*d*₆): 2.54 (s, 6H, 2CH₃), 7.07–7.67 (m, 8H, 2C₆H₄) ppm. ¹²⁵Te NMR (CDCl₃): 266.2 (s) ppm.

Preparation of $[(\mu\text{-}\alpha\text{-C}_{10}\text{H}_7\text{Te})\text{Fe}_2(\text{CO})_6]_2(\mu_4\text{-S})$ (2e**).** The same procedure as that for **2a** was followed, but **1**[MgBr] (R = α -C₁₀H₇) was used instead of **1**[MgBr] (R = Et). From the first main red band was obtained 0.240 g (15%) of $(\mu\text{-}\alpha\text{-C}_{10}\text{H}_7\text{Te})_2\text{Fe}_2(\text{CO})_6$ as a red solid. Mp: $145\text{--}148^\circ\text{C}$. Anal. Calcd for C₂₆H₁₄Fe₄O₁₂Te₂: C, 39.57; H, 1.79. Found: C, 39.29; H, 1.55. IR (KBr disk): $\nu_{\text{C=O}}$ 2060 (s), 2032 (vs), 1988 (vs), 1963 (vs) cm⁻¹. ¹H NMR (CDCl₃): 7.00–8.15 (m, 14H, 2C₁₀H₇) ppm. The second main brown-red band afforded 0.286 g (17%) of **2e** as a dark red solid. Mp: 205°C dec. Anal. Calcd for C₃₂H₁₄Fe₄O₁₂-SeTe₂: C, 34.90; H, 1.28. Found: C, 34.77; H, 1.50. IR (KBr disk): $\nu_{\text{C=O}}$ 2082 (s), 2050 (vs), 2018 (vs), 1993 (vs), 1977 (vs) cm⁻¹. ¹H NMR (CDCl₃): 7.01–8.13 (m, 14H, 2C₁₀H₇) ppm. ¹²⁵Te NMR (CDCl₃): 242.3 (s) ppm.

Standard in Situ Preparation of $[\text{MgX}]^+$ Salts of the Anions $\{(\mu\text{-RS})(\mu\text{-S=CS})[\text{Fe}_2(\text{CO})_6]_2(\mu_4\text{-S})\}^-$ (3**).** A 100 mL two-necked flask equipped with a stir bar, an N₂ inlet tube, and a serum cap was charged with 0.172 g (0.5 mmol) of $\mu\text{-S}_2\text{Fe}_2(\text{CO})_6$ and 20 mL of THF. The resulting red solution was stirred and cooled to -78°C using a dry ice/acetone bath. Into this solution was injected a given amount of RMgX (R = Me, Et, Ph, *p*-MeC₆H₄) in Et₂O by a syringe until the mixture turned to emerald green to give a solution of the $[\text{MgX}]^+$ salts of the anions $\{(\mu\text{-RS})(\mu\text{-S})\text{Fe}_2(\text{CO})_6\}^-$. To this solution was added 0.252 g (0.5 mmol) of Fe₃(CO)₁₂, and then the mixture was warmed to room temperature by removing the dry ice/acetone bath and was stirred at this temperature for 1 h to give a solution of the $[\text{MgX}]^+$ salts of the anions $\{(\mu\text{-RS})(\mu\text{-CO})[\text{Fe}_2(\text{CO})_6]_2(\mu_4\text{-S})\}^-$. To this solution was added 0.10 mL (1.8 mmol) of CS₂, and the mixture was stirred at room temperature for 1 h to give a red-brown solution containing

the salt **3**[MgX] (R = Me, Et, Ph, *p*-MeC₆H₄; X = Br, I), which was immediately used for preparations of **4a–d**.

Preparation of (μ-MeS)[μ-Cp(CO)₂FeSC=S][Fe₂(CO)₆]₂-(μ₄-S) (4a**).** To the above prepared solution of **3**[MgX] (R = Me; X = I) was added 0.152 g (0.5 mmol) of Cp(CO)₂FeI. After the mixture was stirred for 12 h, the solvent was removed under reduced pressure to give a residue, which was subjected to TLC separation using CH₂Cl₂/petroleum ether (2/5 v/v) as eluent. From the main orange-red band 0.161 g (36%) of **4a** was obtained as an orange-red solid. Mp: 145 °C dec. Anal. Calcd for C₂₁H₈Fe₅O₁₄S₄: C, 28.28; H, 0.90. Found: C, 27.98; H, 0.89. IR (KBr disk): ν_{C=O} 2077 (s), 2051 (vs), 2027 (vs), 1991 (vs); ν_{C=S} 1005 (s) cm⁻¹. ¹H NMR (CDCl₃): 2.23 (s, 3H, CH₃), 5.05 (s, 5H, C₅H₅) ppm.

Preparation of (μ-EtS)[μ-Cp(CO)₂FeSC=S][Fe₂(CO)₆]₂-(μ₄-S) (4b**).** The same procedure as that for **4a** was followed, but **3**[MgX] (R = Et; X = Br) was used instead of **3**[MgX] (R = Me; X = I). From the main orange-red band 0.169 g (37%) of **4b** was obtained as a red solid. Mp: 143 °C dec. Anal. Calcd for C₂₂H₁₀Fe₅O₁₄S₄: C, 29.17; H, 1.11. Found: C, 28.99; H, 1.30. IR (KBr disk): ν_{C=O} 2077 (s), 2048 (vs), 2029 (vs), 1987 (vs); ν_{C=S} 1001 (s) cm⁻¹. ¹H NMR (CDCl₃): 1.42 (br s, 3H, CH₃), 2.55 (br s, 2H, CH₂), 5.05 (s, 5H, C₅H₅) ppm.

Preparation of (μ-PhS)[μ-Cp(CO)₂FeSC=S][Fe₂(CO)₆]₂-(μ₄-S) (4c**).** The same procedure as that for **4a** was followed, but **3**[MgX] (R = Ph; X = Br) was used instead of **3**[MgX] (R = Me; X = I). From the main orange-red band 0.178 g (37%) of **4c** was obtained as a red solid. Mp: 154 °C dec. Anal. Calcd for C₂₆H₁₀Fe₅O₁₄S₄: C, 32.74; H, 1.06. Found: C, 32.56; H, 1.04. IR (KBr disk): ν_{C=O} 2078 (s), 2051 (vs), 2032 (vs), 1988 (vs); ν_{C=S} 1006 (s) cm⁻¹. ¹H NMR (acetone-*d*₆): 5.38 (s, 5H, C₅H₅), 7.25–7.65 (m, 5H, C₆H₅) ppm.

Preparation of (μ-*p*-MeC₆H₄S)[μ-Cp(CO)₂FeSC=S][Fe₂(CO)₆]₂-(μ₄-S) (4d**).** The same procedure as that for **4a** was followed, but **3**[MgX] (R = *p*-MeC₆H₄; X = Br) was used instead of **3**[MgX] (R = Me; X = I). From the main orange-red band 0.186 g (38%) of **4d** was obtained as a red solid. Mp: 141 °C dec. Anal. Calcd for C₂₇H₁₂Fe₅O₁₄S₄: C, 33.51; H, 1.25. Found: C, 33.56; H, 1.15. IR (KBr disk): ν_{C=O} 2077 (s), 2053 (vs), 2032 (vs), 1994 (vs); ν_{C=S} 999 (s) cm⁻¹. ¹H NMR (CDCl₃): 2.29 (s, 3H, CH₃), 5.03 (s, 5H, C₅H₅), 7.00–7.45 (m, 4H, C₆H₄) ppm.

Standard in Situ Preparation of [MgX]⁺ Salts of the Anions {[(μ-RS)(μ-S)[Fe₂(CO)₆]₃(μ₄-S)₂}⁻ (5**).** To the [MgX]⁺ salts of the intermediate anions {(μ-RS)(μ-CO)[Fe₂(CO)₆]₂(μ₄-S)}⁻ (R = Me, Ph, *p*-MeC₆H₄; X = Br, I) prepared as described above in the preparation of [MgX]⁺ salts of anions **3** was added 0.172 g (0.5 mmol) of μ-S₂Fe₂(CO)₆. The mixture was stirred for 2 h at room temperature to give a solution containing the salt **5**[MgX] (R = Me, Ph, *p*-MeC₆H₄; X = Br, I), which was utilized in the following preparations for **6a–c**.

Preparation of (μ-MeS)[μ-CpFe(CO)₂S][Fe₂(CO)₆]₃(μ₄-S)₂ (6a**).** To the above prepared solution of **5**[MgX] (R = Me; X = I) was added 0.258 g (0.75 mmol) of Cp(CO)₂FeI. The new mixture was stirred overnight. Solvent was removed under reduced pressure to give a residue, which was subjected to TLC separation using CH₂Cl₂/petroleum ether (1/7 v/v) as eluent. From the main red band 0.123 g (21%) of **6a** was obtained as a black solid. Mp: 162 °C dec. Anal. Calcd for C₂₆H₈Fe₇O₂₀S₄: C, 26.93; H, 0.70. Found: C, 26.50; H, 0.93. IR (KBr disk): ν_{C=O} 2086 (s), 2041 (vs), 1988 (vs) cm⁻¹. ¹H NMR (acetone-*d*₆): 2.32 (s, 3H, CH₃), 5.46 (s, 5H, C₅H₅) ppm.

Preparation of (μ-PhS)[μ-CpFe(CO)₂S][Fe₂(CO)₆]₃(μ₄-S)₂ (6b**).** The same procedure as that for **6a** was followed, but **5**[MgX] (R = Ph; X = Br) was used instead of **5**[MgX] (R = Me; X = I). From the main red band 0.138 g (23%) of **6b** was obtained as a black solid. Mp: 156 °C dec. Anal. Calcd for C₃₁H₁₀Fe₇O₂₀S₄: C, 30.48; H, 0.83. Found: C, 30.20; H, 1.02.

Table 4. Crystal Data and Structural Refinement Details for **2a, **4c**, and **6c****

	2a	4c	6c
mol formula	C ₁₆ H ₁₀ Fe ₄ O ₁₂ STe ₂	C ₂₆ H ₁₀ Fe ₅ O ₁₄ S ₄	C ₃₂ H ₁₂ Fe ₇ O ₂₀ S ₄ ·CH ₂ Cl ₂
mol wt	904.90	953.83	1320.53
cryst syst	triclinic	monoclinic	monoclinic
space group	P $\bar{1}$ (#2)	P2 ₁ /n	P2 ₁ /n
<i>a</i> /Å	9.042(3)	15.9464(16)	9.2669(6)
<i>b</i> /Å	10.046(3)	9.6578(10)	22.5961(15)
<i>c</i> /Å	16.228(6)	23.912(2)	22.5997(14)
α/deg	94.46(3)	90	90
β/deg	105.52(3)	105.178(2)	95.8210(10)
γ/deg	108.87(3)	90	90
<i>V</i> /Å ³	1322.0(9)	3554.2(6)	4707.9(5)
<i>Z</i>	2	4	4
<i>D</i> _c /g cm ⁻³	2.273	1.783	1.863
<i>F</i> (000)	852	1888	2608
abs coeff/mm ⁻¹	4.452	2.289	2.460
temp/K	296	293	293
wavelength/Å	0.710 69	0.710 73	0.710 73
scan type	ω-2θ	ω-2θ	ω-2θ
2θ _{max} /deg	53.9	50.06	50.06
no. of observns	4643	4940	5581
no. of variables	316	442	595
<i>R</i>	0.048	0.0265	0.0453
<i>R</i> _w	0.059	0.0609	0.1240
goodness of fit	1.63	1.008	0.897
largest diff peak/e Å ⁻³	1.45 (near to Te1)	0.369	0.853

IR (KBr disk): ν_{C=O} 2060 (s), 2040 (vs), 1998 (vs) cm⁻¹. ¹H NMR (acetone-*d*₆): 5.48 (s, 5H, C₅H₅), 7.33–7.51 (m, 5H, C₆H₅) ppm.

Preparation of (μ-*p*-MeC₆H₄S)[μ-CpFe(CO)₂S][Fe₂(CO)₆]₃(μ₄-S)₂ (6c**).** The same procedure as that for **6a** was followed, except that **5**[MgX] (R = *p*-MeC₆H₄; X = Br) was used instead of **5**[MgX] (R = Me; X = I). From the main red band 0.182 g (29%) of **6c** was obtained as a black solid. Mp: 160 °C dec. Anal. Calcd for C₃₂H₁₂Fe₇O₂₀S₄: C, 31.11; H, 0.98. Found: C, 30.96; H, 1.08. IR (KBr disk): ν_{C=O} 2056 (s), 2038 (vs), 1997 (vs) cm⁻¹. ¹H NMR (CDCl₃): 2.29 (s, 3H, CH₃), 5.48 (s, 5H, C₅H₅), 7.15, 7.19, 7.37, 7.41 (q, AA'BB', 4H, C₆H₄) ppm.

X-ray Structure Determinations of **2a, **4c**, and **6c**.** Single crystals of **2a**, **4c**, and **6c** suitable for X-ray diffraction analyses were grown by slow evaporation of their CH₂Cl₂/hexane solutions at about 4 °C. Each crystal was mounted on an Enraf-Nonius CAD4 or a Bruker SMART 1000 automated diffractometer with a graphite monochromator with Mo Kα radiation (λ = 0.710 69 or 0.710 73 Å). The structures were solved by direct methods and expanded by Fourier techniques. The final refinements were accomplished by the full-matrix least-squares method with anisotropic thermal parameters for non-hydrogen atoms. Hydrogen atoms were located by using the geometric method. The calculations were performed using the TEXSAN crystallographic software package of the Molecular Structure Corp. for **2a** and the SHELXTL-97 program for **4c** and **6c**. Details of the crystal data, data collections, and structure refinements are summarized in Table 4.

Acknowledgment. We are grateful to the National Natural Science Foundation of China and the State Key Laboratory of Organometallic Chemistry for financial support.

Supporting Information Available: Full tables of crystal data, atomic coordinates and thermal parameters, and bond lengths and angles for **2a**, **4c**, and **6c**. This material is available free of charge via the Internet at <http://pubs.acs.org>.

OM011039V